RAPID COMMUNICATIONS

PHYSICAL REVIEW A VOLUME 47, NUMBER 4 APRIL 1993

Measurements of light-scattering noise accompanying two-wave mixing in a Kerr medium

R. Pizzoferrato, U. Zammit, and M. Marinelli
Dipartimento Ingegneria Meccanica, II Università di Roma "Tor Vergata," Via E. Carnevale, 00173 Roma, Italy

R. McGraw and D. Rogovin
Rockwell International Science Center, 1049 Camino Dos Rios, Thousand Oaks, California

(Received 29 June 1992)

We report measurements of noise accompanying two-wave mixing in a Kerr medium. Experiments were conducted at visible wavelengths using an aqueous suspension of shaped microparticles as the nonlinear medium. Theoretical calculations and computer simulations using a stochastic model for light-scattering noise are shown to give excellent agreement with the experimental results.

PACS number(s): 42.65.Hw, 05.40.+j, 78.35.+c

The propagation and mixing of electromagnetic waves in Kerr media have been studied since the earliest days of nonlinear optics [1] and continue to be a focus of considerable research interest. Specific applications include optical phase conjugation via four-wave mixing [2], squeezed-light generation [3], and two-wave mixing [4]. In all of these processes, noise is an important consideration. Recent studies based on the fluctuation-dissipation theorem have shown that the optical Kerr coefficient is fundamentally associated with thermal fluctuations in the linear dielectric constant of the medium. These fluctuations reduce the fidelity of an optical signal by mixing in scattered light from the pump-laser field as noise [5,6]. In this Rapid Communication we report measurements of noise during two-wave mixing in a Kerr medium and demonstrate excellent agreement with theoretical predictions for thermal light-scattering noise [7].

Measurements of gain and noise were made using liquid suspensions of polytetrafluoroethylene (PTFE) shaped microparticles as artificial Kerr media. Light-induced, particle-orientation rearrangements account for optically induced birefringence with consequent large nonlinear optical response. Several studies have been carried out to characterize the linear and nonlinear optical properties of these suspensions, and good agreement between theoretical predictions and experimental results was found [8–10]. This agreement is due in large part to the characteristics of the suspensions, which fit an independent-particle single orientational relaxation-time Debye model remakably well. Particles are ellipsoidal in shape (the dimensions are $0.4\times0.2\times0.2\ \mu m^3$) and the particle polarizability tensor has corresponding symmetry. The particle suspensions are highly monodisperse and interparticle interactions are negligible even at relatively high volume fractions (1.0–2%). In the present experiments we typically used a 1% volume fraction of PTFE particles suspended in a 65-35 water-glycerol host-liquid mixture. This mixture was chosen because it matches the average value of the particle refractive index $n_0=1.376$, thus minimizing the importance of light-scattering fluctuations due to the isotropic part of the particle polarizability (8).

Figure 1 shows the experimental setup for nondegenerate two-wave mixing. The pump and the probe waves are provided by splitting the 514-nm TEM_{00} output of a cw argon-ion laser into a 1-W-power pump beam and a 50-mW probe beam. The two beams eventually intersect at the focus of the lens (L) within the sample at an angle of 5°. The beam waist size is about 100 μm and the interaction length is 0.1 cm. Before entering the sample, the polarization direction of the pump beam is rotated perpendicular to that of the probe so that only the orientational-particle gratings are generated in the suspension by the beam interference pattern [10].

The angular frequency shift Ω required for the nondegenerate beam configuration is provided to the pump beam by the mirror M1 that is mounted to a piezoelectric transducer (PZT). A triangular 8-Hz high-voltage wave is fed through the PZT so as to produce a periodic linear displacement of the mirror with constant, sign-inverting speed. The consequent square-wave-like angular frequency shift can be varied by either changing the amplitude or the frequency of the mirror displacement. The periodic

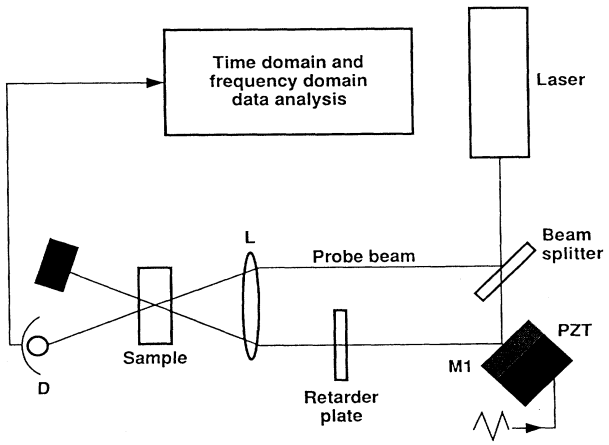

FIG. 1. Schematic diagram of the two-wave mixing optical arrangement and electronics for noise analysis. L, focusing lens; M1, 100% mirror; PZT, piezoelectric transducer; D, photodiode.

intensity gain of the probe beam is revealed by a low-noise photodiode (D). A polarizer is placed before the photodiode to remove the polarized component of the pump light scattered into the probe beam by the isotropic particle fluctuations. After a low-pass electrical amplification (−3 dB at 3 kHz), the photodiode output is fed both into a digital oscilloscope and into a 12-bit, computer-interfaced spectrum analyzer. For each value of the frequency shift, the average value of the intensity gain was obtained by a digital average on the oscilloscope while the spectral properties of the gain fluctuations were monitored on the spectrum analyzer.

Implementing this setup, particular care had to be taken to damp mechanical vibrations that could add random phase shifts to the beams, thus introducing spurious noise in the gain process.

Figure 2(a) shows the experimental results for the probe intensity gain and noise fluctuations. Pump light intensity in the sample was approximately 10 kW/cm^2, while the transmitted probe power in the absence of the pump beam was 50 mW. The vertical bars report the transmitted probe-beam power in watts as a function of the nondimensional frequency shift $\Omega\tau$, where $\tau=\tau_R=8,9$ ms is the orientational response time as determined through independent measurements [10]. Each vertical bar is centered on the average value of the transmitted power and the bar length reports the root-mean-square (rms) value of the noise fluctuations on the same scale. rms noise fluctuations are also shown in the figure on an expanded scale for clarity (full circles) and were obtained by integration of the noise power spectrum over a collection bandwidth of 60 Hz. The smooth curve is a fit to the data using $\sigma(P_2)=C[1+(\Omega\tau)^2]^{-1/2}$, which is the form expected from the theory, which will now be described.

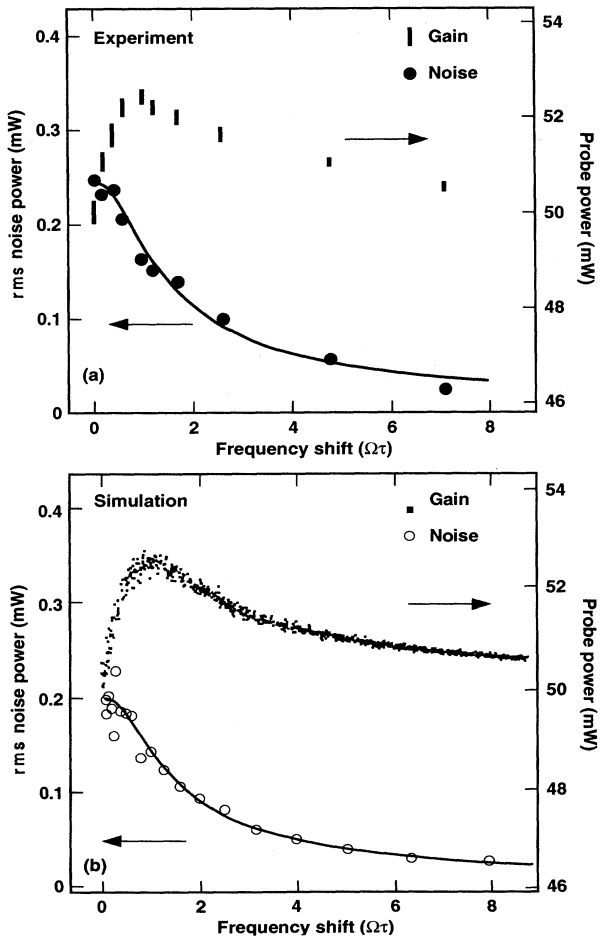

FIG. 2. Comparison of experimental and simulation results for two-wave mixing gain and light-scattering noise.

For two incident plane waves the total field is of the form

$$\mathbf{E}(\mathbf{r},t)=\mathbf{e}_1E_1(\mathbf{r})\cos[\mathbf{K}_1\cdot\mathbf{r}-\omega_1t+\theta_1(\mathbf{r})] +\mathbf{e}_2E_2(\mathbf{r})\cos[\mathbf{K}_2\cdot\mathbf{r}-\omega_2t+\theta_2(\mathbf{r})]\ , \quad (1)$$

where $\mathbf{e}_j$, $E_j(\mathbf{r})$, and $\theta_j(\mathbf{r})$ are the unit polarization vector, slowing varying amplitude, and slowly varying phase of wave j, respectively. Inserting Eq. (1) into the wave equation, making the slowly varying amplitude and phase approximation, and equating the in-phase and out-of-phase terms gives a set of four coupled equations describing the evolution of the two amplitudes and two phases, which may be integrated using the stochastic noise model [6,7]. In the absence of pump depletion and background loss, an analytic solution to these equations may be obtained, which is sufficient for comparison with the present measurements. Here we require the solution for the weak probe beam $E_2(L)$, where L is the beam interaction length, in the presence of a nondepleted pump E_1. The result, from Ref. [7], is

$$E_2(L)=\exp(\alpha_sL)E_2(0)+(\alpha_N/\alpha_S)[\exp(\alpha_SL)-1]E_1\ , \quad (2)$$

where

$$\alpha_S=(K/4\varepsilon_0)\varepsilon_2E_1^2\Omega\tau/[1+(\Omega\tau)^2=h\Omega\tau/[1+(\Omega\tau)^2] \quad (3)$$

and

$$\alpha_N=(K/4\varepsilon_0)b_\Omega\ . \quad (4)$$

In Eq. (3), $K=|\mathbf{K}_1|=|\mathbf{K}_2|$, ε_0 is the background dielectric constant, ε_2 is the Kerr coefficient, and $\Omega=\omega_1-\omega_2$. The last equality in Eq. (3) defines h. In Eq. (4), b_Ω is the quadrature component for a thermal fluctuation grating having the same orientational configuration as the signal grating, thereby giving rise to a scattered light component that is indistinguishable from the signal beam (7). Note that ε_2 and b_Ω are off-diagonal components of second-rank tensors, but may be treated here as scalars since in each case only one tensor component is selected by the fixed polarizations of the writing beams.

Inspection of Eqs (2)–(4) reveals that fluctuations in b_Ω cause fluctuations in the amplitude of the transmitted probe. In addition to b_Ω, there is an in-phase noise component a_Ω, which results in fluctuations in the phase. The mean and variances for the grating amplitude fluctuations are derived in Ref. [7],

$$\langle a_\Omega \rangle = \langle b_\Omega \rangle = 0 \ , \tag{5a}$$

$$\langle a_\Omega^2 \rangle = \langle b_\Omega^2 \rangle = (2\tau B)\langle |\delta\varepsilon(\mathbf{q})|^2 \rangle / [1+(\Omega\tau)^2] \ , \tag{5b}$$

where the dependence on frequency difference Ω and response time τ follows our assumption of a single relaxation-time Debye medium. The right-hand side of Eq. (5b) gives the noise power over a frequency bandwidth B and is obtained by multiplying the result of Ref. [7], which gives the noise power on a per unit angular frequency basis, by $2\pi B$. The right-hand side of Eq. (5b) may be evaluated in terms of the nonlinear dielectric constant, or Kerr coefficient, ϵ_2 using [5,6]

$$\langle |\delta\epsilon(\mathbf{q})|^2 \rangle = 8\pi k T \epsilon_2 / V_s \ , \tag{6}$$

where $\mathbf{q}=\mathbf{K}_1-\mathbf{K}_2$ is the wave vector of the matched thermal fluctuation grating and V_s is the scattering or beam interaction volume determined from the product of the beam cross-section area A and the interaction length L.

For comparison with experiment, Eq. (2) was evaluated numerically using the stochastic noise model (6). The one adjustable parameter in the theory is the Kerr coefficient, and this is obtained here from a fit to the gain curve, not to the noise. The gain curve shown in Fig. 2(b) was obtained using $\epsilon_2 = 3.6\times10^{-7}$ cm^3/erg, in reasonable agreement with the estimate for this quantity obtained from previous nonlinear optics measurements [8–10]: $\epsilon_2 = 2.5\times10^{-7}$ cm^3/erg. The remaining conditions used in the calculations are the same as those described above for the experiment. The simulation proceeds by the following steps. (i) A value for $\Omega\tau$ is selected and Eqs. (5) are used to obtain the mean and variance for the noise amplitude fluctuations over the measurement bandwidth $B=60$ Hz. The fluctuations are assumed to be Gaussian and sampling is achieved using a standard computer algorithm incorporating the Box-Muller transformation for the generation of normal deviates from random numbers sampled uniformly on the interval (0,1). (ii) Equation (2) is evaluated for each sampled b_Ω to give a solution for $E_2(L)$ and corresponding amplified signal power $P_2(L)$. Steps (i) and (ii) are repeated on the order of a thousand times to obtain a good statistical sampling of the noise over the full $\Omega\tau$ range of interest. Results of the calculation are shown in Fig. 2(b). Note that both the experimental and theoretical gain profiles follow frequency dispersion curves characteristic of the Debye relaxation model [8,10]. More importantly, there is excellent agreement between theory and experiment in regard to the rms values of the noise fluctuations, including their dependence on frequency shift. This agreement is remarkable, in view of the lack of adjustable parameters in the theory.

Squaring the right-hand side of Eq. (2) gives noise terms proportional to α_N and to α_N^2. In most cases of interest, $E_2(0)$ is sufficiently large that the latter term may be neglected, leaving the cross term containing the product $E_1E_2(0)$. Then we find for the standard deviation of the power fluctuations in the amplified signal in the limit of small gain [7],

$$\sigma(P_2) = (4\pi\tau B)^{1/2}(hL)^{1/2}[kT\nu P_2(0)]^{1/2} \times [1+(\Omega\tau)^2]^{-1/2} \quad (hL \ll 1) \ . \tag{7}$$

Since the maximum power gain ($G=e^{hL}$) in the experiment is 1.05, the small gain approximation used to derive Eq. (7) is valid for the present discussion. Equation (7) shows the origin of the $[1+(\Omega\tau)^2]^{-1/2}$ dependence seen in the measurements and provides an explicit form for the prefactor C. Here $P_2(0)$ is the incident signal power, P_2 is the fluctuating signal power at $z=L$, and $\sigma(P_2)$ is the standard deviation of P_2: $\sigma(P_2)=[\langle (P_2)^2 \rangle - \langle P_2 \rangle^2]^{1/2}$.

The solid curve in Fig. 2(b) displays the analytical result given by Eq. (7). The open circles are numerical results obtained by Gaussian sampling using the stochastic noise model—each circle represents the rms value computed for 100 samples at a fixed value of $\Omega\tau$. The simulated noise is in excellent agreement with both the analytical and experimental results. Finally, we note that the noise fluctuations decrease monotonically with frequency unlike the average gain, which peaks at $\Omega\tau=1$.

Equation (7) shows that the rms amplitude of the noise fluctuations increases with the square root of the incident probe power $P_2(0)$. Figure 3 reports the experimental values of the rms noise power (triangles) as a function of the probe power for $\Omega\tau=0$. As can be seen, the square-root dependence (full line) is well verified over a decade range.

Theory predicts that the rms probe-power fluctuations should satisfy Eq. (7) as long as light-induced gratings are dominant with respect to thermal gratings. Equation (2) shows that for an incident probe power of zero, output fluctuations will occur proportional to α_N^2. Note that the noise fluctuations proportional to α_N^2, unlike those proportional to α_N, do not vanish on time averaging. Analysis similar to that used to derive Eq. (7) gives

$$\langle P_2(L) \rangle = (\pi\tau B)(hL)(kT\nu)[1+(\Omega\tau)^2]^{-1} \ , \tag{8}$$

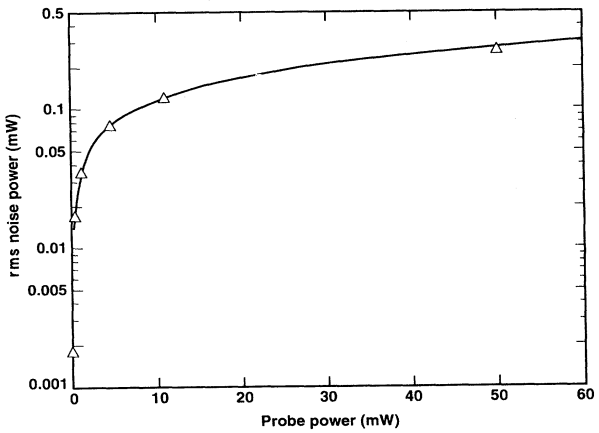

FIG. 3. rms noise power as a function of probe power for $\Omega\tau=0$. The experimental data points (triangles) follow a square-root dependence on the probe power (solid curve) as predicted from Eq. (7). The single data point on the ordinate gives the rms noise power measured in the absence of the probe beam as discussed in connection with Eq. (8).

where $\langle P_2(L) \rangle$ is the average power of the noise at $z = L$. The factor $(kT\nu)$ is the Nyquist expression for the thermal noise power radiated by a channel having a bandwidth equal to the optical frequency ν. Equation (8) yields a predicted average noise power at zero probe power of 0.2 μW due entirely to scattered pump light. The stochastic noise model sampling confirms this result and gives an rms power of 0.28 μW. The rms noise power was measured at zero signal power by blocking the probe. The result of this measurement (1.8 μW rms) is represented by the single data point appearing on the ordinate of Fig. 3. At this low-noise level, the discrepancy between theory and experiment is much greater than for the previous comparisons made with the probe beam on and most likely due to extraneous sources of noise being present in the measurement.

The results described in this Rapid Communication apply to the thermal noise limit ($\Omega \ll kT/\hbar$) typical of slow media having large nonlinear optical coefficients. In this limit the maximum frequency difference Ω is limited by the medium response time and quantum noise effects, which can be dominant for Raman amplifiers [11], may be neglected. Excellent agreement between experiment and theoretical calculations based on the stochastic model of thermal light-scattering noise has been obtained. A future paper will extend the theory to fast response media, for which Ω is comparable to or greater than $kT/\hbar$, in a unified treatment of quantum-thermal noise.

Note added. After our experiments had been completed, a paper by Sternklar, Glick, and Jackel examined noise limitations for Brillouin two-beam coupling [12], which also confirms a number of predictions from Ref. [5]. In addition to the focus on Brillouin two-beam coupling, two important differences between Ref. [12] and the present study are the following: (i) Ref. [12] does not treat the dependence of noise on the frequency difference between the two beams, and (ii) it does not treat the noise fluctuation term proportional to our α_N, but only the term proportional to our α_N^2 that does not vanish on time averaging.

The authors thank Dionisio Del Vescovo for his advice concerning experimental data analysis of noise. R.M. and D.R. gratefully acknowledge theoretical work supported by the U.S. Air Force under Contract No. F29601-89-C-0085.

[1] N. Bloembergen, *Nonlinear Optics* (Benjamin, New York, 1965).

[2] *Optical Phase Conjugation*, edited by R. A. Fisher (Academic, New York, 1983).

[3] R. Shelby, M. D. Levenson, S. H. Perlmutter, R. G. DeVoe, and D. F. Walls, Phys. Rev. Lett. **57**, 691 (1986).

[4] Y. Silberberg and I. Bar-Joseph, J. Opt. Soc. Am. B **1**, 662 (1984).

[5] R. McGraw, D. Rogovin, and A. Gavrielides, Appl. Phys. Lett. **54**, 199 (1989).

[6] R. McGraw, Phys. Rev. A **45**, 3250 (1992).

[7] R. McGraw, J. Opt. Soc. Am. B **9**, 98 (1992).

[8] R. Pizzoferrato, D. Rogovin, and J. Scholl, Opt. Lett. **16**, 297 (1991).

[9] M. De Spirito, R. Pizzoferrato, M. Marinelli, U. Zammit, D. Rogovin, R. McGraw, and J. Scholl, Opt. Lett. **16**, 120 (1991).

[10] D. Rogovin, J. Scholl, R. Pizzoferrato, M. De Spirito, U. Zammit, and M. Marinelli, Phys. Rev. A **44**, 7580 (1991).

[11] R. C. Swanson, P. R. Battle, and J. L. Carlsten, Phys. Rev. A **45**, 1932 (1992).

[12] S. Sternklar, Y. Glick, and S. Jackel, J. Opt. Soc. Am. B **9**, 391 (1992).